

Analysis of Process Configurations for CO₂ Capture by Precipitating Amino Acid Solvents

Eva Sanchez-Fernandez,^{*,†} Katarzyna Heffernan,[†] Leen van der Ham,[†] Marco J. G. Linders,[†] D. W. F. Brillman,[‡] Earl L. V. Goetheer,[†] and Thijs J. H. Vlugt[§]

[†]TNO, Netherlands organization for applied scientific research, Leeghwaterstraat 46, 2628CA Delft, The Netherlands

[‡]University of Twente, TNW/TCCB Meander 222, 7500 AE Enschede, The Netherlands

[§]Delft University of Technology, Process and Energy Department, Leeghwaterstraat 39, 2628CB Delft, The Netherlands

S Supporting Information

ABSTRACT: Precipitating amino acid solvents are an alternative to conventional amine scrubbing for CO₂ capture from flue gas. Process operation with these solvents leads to the formation of precipitates during absorption that need to be re-dissolved prior to desorption of CO₂. The process configuration is crucial for the successful application of these solvents. Different process configurations have been analyzed in this work, including a full analysis of the baseline operating conditions (based on potassium taurate), the addition of lean vapor compression, multiple absorber feeds, and the use of different amino acids as alternative solvents to the baseline based on potassium taurate. The analysis is carried out with an equilibrium model of the process that approximates the thermodynamics of the solvents considered. The results show that the precipitating amino acid solvents can reduce the reboiler duty needed to regenerate the solvent with respect to a conventional MEA process. However, this reduction is accompanied by an expenditure in lower grade energy needed to dissolve the precipitates. To successfully implement these processes into power plants, an internal recycle of the rich stream is necessary. This configuration, known as DECAB Plus, can lower the overall energy use of the capture process, which includes the energy needed to regenerate the solvent, the energy needed to dissolve the precipitates, and the energy needed to compress the CO₂ to 110 bar. With respect to the energy efficiency, the DECAB Plus with lean vapor compression configuration is the best configuration based on potassium taurate, which reduces the reboiler duty for regeneration by 45% with respect to conventional MEA. Retrofitting this process into a coal fired power plant will result in overall energy savings of 15% with respect to the conventional MEA process, including compression of the CO₂ stream to 110 bar. Potassium alanate was found to reduce the energy use with respect to potassium taurate under similar process configurations. Therefore, the investigation of potassium alanate in a DECAB Plus configuration is highly recommended, since it can reduce the energy requirements of the best process configuration based on potassium taurate.

1. INTRODUCTION

CO₂ capture based on absorption and thermal desorption on a large scale is considered a suitable technology for carbon abatement in the current energy sector (highly dependent on fossil fuels).^{1–3} Major drawbacks of this technology are the efficiency penalties and high operating cost, related to solvent regeneration and CO₂ compression, which prevent commercial application at large scale.^{4–6} The integration of CO₂ capture into power plants results in a reduction of the net power plant efficiency which depends on the capture technology, power plant type, and degree of heat integration.^{5,7–10} Amine solvents are the most common industrial choice for low pressure absorption.^{11–13} In the case of coal fired power plants, reductions of plant efficiencies of 9–12 percentage points are expected for the conventional industrial standard monoethanolamine (MEA).^{14–16} MEA is also degraded in the presence of SO₂, O₂, and metal ions in solution with the formation of irreversible byproducts or degradation products,¹⁷ reducing the absorption capacity of the amine and increasing the emissions of undesirable products to the atmosphere.¹⁸

Improvements to the costs of the conventional industrial standard (30 wt % MEA solution) can be obtained by screening for solvents that have higher absorption capacity and rates (e.g.,

promoted tertiary amines and hindered amines such as promoted MDEA).^{19–22} Improvements, both economically and environmentally, can also be made by developing solvents with a higher resistance to degradation and lower toxicity and volatility. Alternative solvents to amines are amino acid salts²³ and promoted potassium carbonate.^{24–26} Besides the solvents suited for the conventional absorption–desorption process, other solvents that are under development are the phase change systems such as the carbonate precipitating processes,²⁷ the demixing solvent technology,²⁸ and precipitating amino acid salts.²⁹ Alternative process configurations have also been proposed to reduce capital and operating costs of the CO₂ capture process.³⁰ Numerous publications propose flow-sheet modifications to the conventional MEA industrial process in order to upgrade the process or its energetic integration with the steam cycle of the power plant.^{31–34} Frequent configurations to be evaluated are the modification of process operating conditions (e.g., stripper process conditions, lean-rich

Received: July 20, 2013

Revised: October 13, 2013

Accepted: November 27, 2013

Published: November 27, 2013

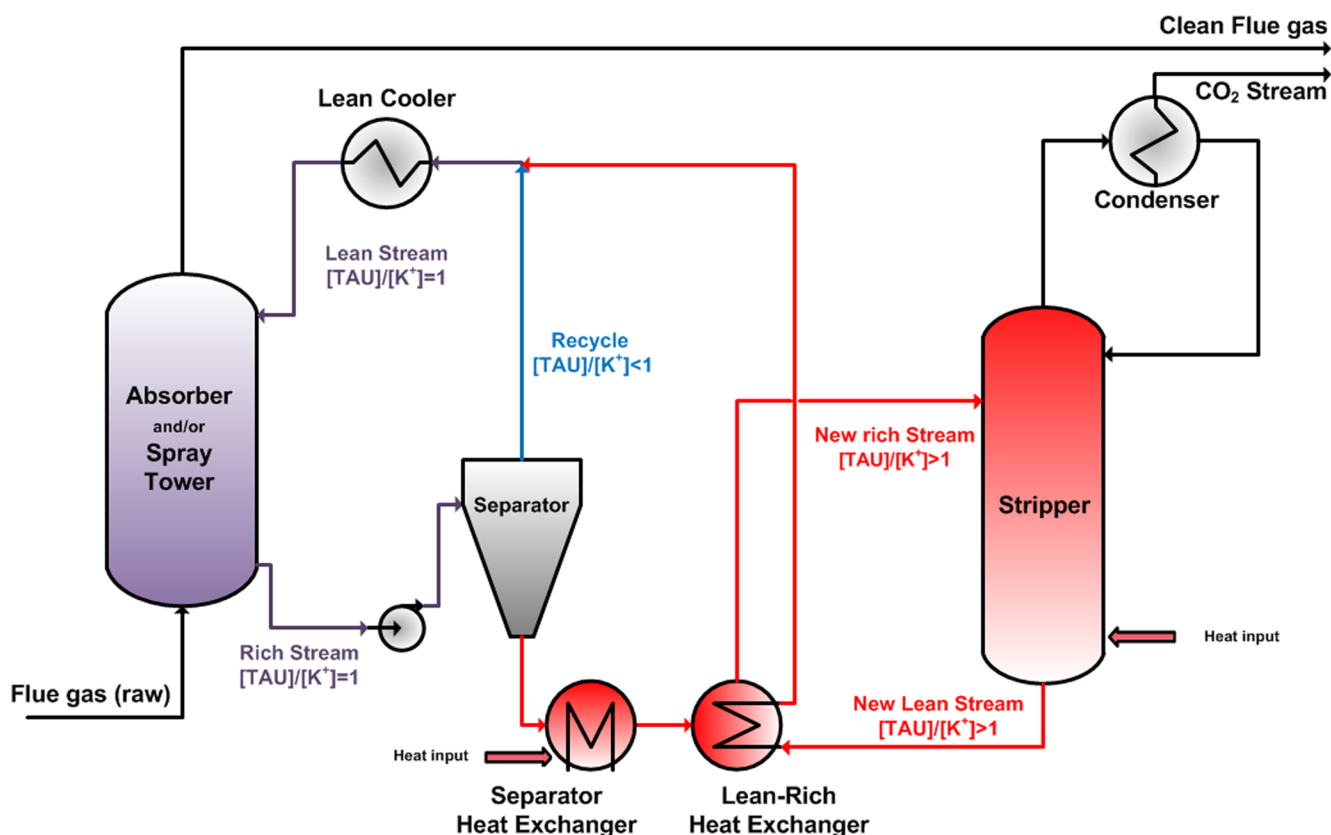


Figure 1. DECAB and DECAB Plus process concepts based on precipitating potassium taurate. The separator and recycle stream are only pertinent for the DECAB Plus concept. DECAB can be seen as a simplification of this flowsheet where the recycle stream is set to zero. The ratio of the total taurine concentration to the total potassium concentration in solution is indicated below the name of each stream. This ratio can be 1 (equimolar solution), higher than 1 (solution with less potassium than the equimolar solution and, therefore, lower pH_0), or less than 1 (solution with more potassium than the equimolar solution and, therefore, higher pH_0).

heat exchanger pinch),³⁵ the use of multiple absorber feeds or staged feed to the stripper (e.g., the split flow scheme),³⁶ and the use of the sensible heat contained in the exit streams of the stripper column (e.g., the lean vapor compression configuration).³⁷

Precipitating amino acid solvents are a promising alternative to amines. In specific cases, a lower energy required to regenerate the solvent has been reported.³⁸ Other benefits when compared to MEA are higher stability and lower corrosion in the case of taurine,³⁹ higher absorption rates in the case of sarcosine,⁴⁰ and proline.⁴¹ Due to the non-volatile nature of these solvents, lower emissions are foreseen for processes based on precipitating amino acids. The simplest process configuration based on these solvents (DECAB) requires the use of a spray tower to handle solids during absorption. The precipitates are re-dissolved before desorption, which takes place in a conventional stripper.²⁹ The introduction of an internal recycle in this process configuration (DECAB Plus) can enhance the release of CO_2 without modifications in the stripper.³⁸

In this work, an evaluation and optimization of different process configurations based on the precipitating amino acid solvents is presented. The evaluation has focused on two research directions: improvements in process configuration and screening for alternative solvents with improved performance. The evaluation relies on an equilibrium based model, which includes all the necessary unit operations of the processes to capture CO_2 from coal fired power plants' flue gas. The model

uses an approximate thermodynamic representation of the solvents investigated on the basis of empirical correlations that have been derived from experimental data. Initially, an investigation of DECAB and DECAB Plus process conditions is presented on the basis of potassium taurate. The key parameters of the processes are modified with the objective of decreasing the required energy for regeneration. After optimizing the process conditions, two process additions are integrated and investigated. These include the lean vapor compression option and multiple feeds to the absorber. The performance of other amino acid solvents is also investigated for the DECAB process configuration.

2. BASELINE CONFIGURATION (DECAB AND DECAB PLUS)

CO_2 absorption in aqueous amino acid salt solutions generally leads to the formation of precipitates, depending on the particular amino acid and the concentration in solution.^{42,43} The composition of the precipitates varies with the structure of the amino acid used to prepare the amino acid salt solution. It can contain mainly the pure amino acid, for primary amino acids, KHCO_3 , for highly hindered amino acids, or a combination of amino acid and KHCO_3 , for other amino acids.⁴³ This phase change can influence the equilibrium reactions in CO_2 absorption and desorption contributing to reduce the energy use of the conventional absorption-desorption capture process. The chemistry of the reaction of CO_2 with amino acid salts in the precipitation regime has been

described by Kumar.⁴⁴ The identified effects related to precipitation are the following: (1) the enhancement of the specific CO₂ capacity of amino acid salt solutions;⁴⁵ (2) the acidification of the rich solution, which is not a direct effect of precipitation but is brought about by introducing a phase separation after precipitation that partially removes the supernatant and results in the concentration of the amino acid in the rich solution once the precipitates have been re-dissolved.^{46,47} The first effect, enhancement of CO₂ absorption, occurs when precipitates are formed during absorption as a result of the chemical reaction of CO₂ with the amino acid salt. The products of this reaction that have a limited solubility (the pure amino acid and/or the KHCO₃) precipitate when the saturation point is reached. The removal of the solid reaction product from the liquid phase shifts the reaction equilibrium toward the production of more products. The result is a rich stream in the form of slurry that contains mainly the pure amino acid in the solid phase (for primary amino acids) or a mixture of pure amino acid and bicarbonate (for more hindered amino acids) and carbamate, bicarbonate, amino acid salt counterion (e.g., potassium, sodium), and remaining amino acid species in the liquid phase. The second effect, acidification of the rich stream, requires the processing of the slurry in a solid–liquid separator to partially separate the supernatant from the solids. This forms a concentrated slurry, which is heated to dissolve the amino acid precipitates. The resulting rich solution, enriched in amino acid, is further processed in the stripper for desorption. The supernatant excess, enriched in amino acid salt counterions, is recycled to the absorber without passing through the stripper. After dissolving the amino acid crystals, the pH of the rich stream is decreased before thermal desorption, enhancing the release of the chemically bonded CO₂.

Figure 1 illustrates a generic precipitating amino acid process scheme based on the potassium salt of taurine that exploits both effects. The flue gas, containing ca. 13% v/v CO₂ at 40 °C, is treated with a solution of potassium taurate with 1:1 molar amounts of taurine and KOH in a suitable contactor that can handle solids. This can be a spray tower contactor or a sequence of spray tower contactor and packed column.²⁹ The slurry that results from the absorption of CO₂ can be directly regenerated in the stripper, via the lean-rich heat exchanger, in a process concept known as DECAB.²⁹ In this case, the separator in Figure 1 is not needed. Alternatively, the slurry can be treated in the solid–liquid separator, yielding two streams: new rich stream and recycle. The new rich stream is a slurry enriched in taurine, that has a taurine-to-potassium molar ratio ([TAU/K]) higher than 1. This stream is further processed in the stripper, where the CO₂ is released, yielding the new lean stream. By re-dissolving the amino acid crystals, the pH of the new rich solution is decreased before thermal desorption, which results in higher partial pressures of CO₂ under stripper conditions that facilitate desorption. The recycle stream is the supernatant excess enriched in potassium ions, that has a taurine-to-potassium molar ratio lower than 1. This stream is mixed with the new lean stream and is fed back to the absorber without passing through the stripper. Mixing the recycle and the new lean stream results in the initial lean stream that has a taurine-to-potassium molar ratio of 1. This process alternative is known as DECAB Plus.

The technical analysis of these process concepts with potassium taurate presented in our previous work⁴⁷ shows that the DECAB process concept can decrease the reboiler duty

needed for solvent regeneration. Compared to a conventional MEA process, the reboiler duty of the DECAB process concept is 10% lower. This duty can be further reduced with the DECAB Plus concept. Due to the internal recycle in this process concept, the rich stream that is regenerated in the stripper has a substantially higher CO₂ equilibrium pressure due to the pH change that is induced by concentrating the amino acid. For this reason, a “super lean” stream is obtained in the stripper with less energy penalty. At the same time, the recycled stream that is fed back to the absorber contains a high concentration of CO₂, which decreases the process capacity. With an optimum recycle, the first effect is dominant, resulting in a 35% lower reboiler duty compared to a conventional MEA process.⁴⁷ Other effects of the internal recycle, which are linked to the change of amino acid speciation due to a lower pH, are the reduction in the heat of desorption and the reduction of the amino acid solubility in the new rich stream. The first effect contributes substantially to the reduction in regeneration energy, but the second effect limits the extension of the internal recycle (and its benefits) to avoid solids in the new rich stream that is fed to the stripper. Another point of attention is that DECAB and DECAB Plus processes require the input of low-grade energy to re-dissolve the solids formed during absorption. The energy needed for this phase change is approximated by the dissolution energy and is supplied to the new rich stream in the separator heat exchanger (Figure 1). This energy is of a relatively low quality compared to the steam quality required by the reboiler, and it could be supplied by low pressure steam (ca. 1 bar), hot water of about 80 °C, or stripper reboiler condensate. However, in the case of potassium taurate, it is substantial in terms of volume, due to the high heat of dissolution of this amino acid salt.⁴⁷ For future development of these processes, the main points for improvement are the net capacity of the solvent, which becomes a dominant factor when high portions of the rich stream are recycled, the solubility of the amino acid, and the heat of dissolution of the amino acid.

3. ALTERNATIVE PROCESS CONFIGURATIONS FOR DECAB AND DECAB PLUS

The use of alternative process configurations or solvents could further reduce the energy requirements of DECAB and DECAB Plus processes. The main focus for process improvement is the selection of process conditions that maximize process capacity, which in turn will minimize the energy required by the reboiler for solvent regeneration. Moreover, the energy required by the separator heat exchanger to re-dissolve the crystals is linked to the required solvent flow rate, which depends on the solvent net capacity. Therefore, increasing the bulk solvent capacity will also reduce the energy requirements of the separator heat exchanger. The process modifications that have been analyzed in this work are intended to improve the process capacity of the DECAB and DECAB Plus process concepts. The selected process modifications are as follows: (1) optimization of the operating conditions of the baselines, (2) the introduction of the lean vapor compression (LVC) configuration, (3) the use of multiple feeds to the absorber, and (4) the use of an alternative amino acid solvent to potassium taurate. These options are discussed in the following sections.

3.1. Optimization of the Operating Conditions of DECAB and DECAB Plus. The modifications to the process operating conditions of the baselines have the objective of optimizing the combined thermal and pH-shift effects during

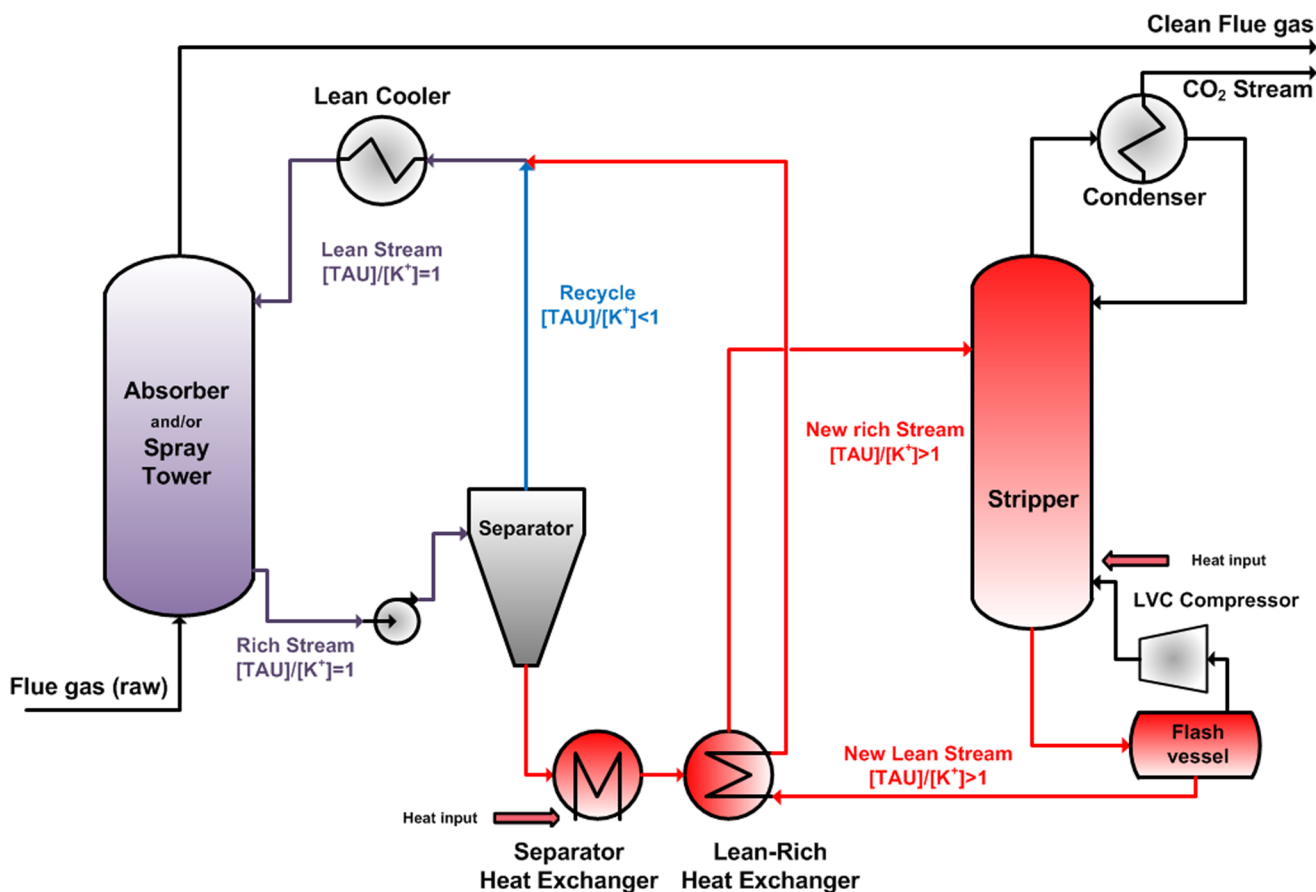


Figure 2. DECAB Plus process based on precipitating potassium taurate with LVC. The ratio of the total taurine concentration to the total potassium concentration in solution is indicated below the name of each stream. This ratio can be 1 (equimolar solution), higher than 1 (solution with less potassium than the equimolar solution and, therefore, lower pH_0), or less than 1 (solution with more potassium than the equimolar solution and, therefore, higher pH_0).

desorption. The thermal effect depends on the operating temperature of the reboiler, and the pH-shift effect depends on the amount of precipitate that is formed during absorption, the temperature at which the solid–liquid separation takes place, and the fraction of the liquid supernatant that is recycled. For the purpose of optimization, the reboiler temperature, the separator temperature, and the flow of the recycle stream have been modified to analyze the combined effect of temperature and different $[\text{TAU}/\text{K}]$ ratios on the reboiler duty.

3.2. Lean Vapor Compression (LVC). The LVC option has been described and investigated for other solvent systems, such as MEA.^{32,33,35,37,48} In this process concept, illustrated in Figure 2, the lean stream that leaves the stripper column is flashed adiabatically in a separate vessel. As a consequence of the pressure reduction, the solvent is partially evaporated. The vapor generated is recompressed and reinjected at the base of the stripper column. The benefits of this process concept are that part of the CO_2 remaining in the lean stream is flashed, reducing the lean loading, and that more steam is generated, reducing the necessary heat input to the reboiler.

3.3. Multiple Feeds to the Absorber. The DECAB Plus process concept with multiple feeds to the absorber is illustrated in Figure 3. In this configuration, the new lean stream that leaves the stripper column is divided into two streams. One of the streams is mixed with a fraction of the recycle stream and fed to the top of the absorber column. The other stream is mixed with the remaining fraction of the recycle

stream and is fed at an intermediate stage within the absorber column. This alternative configuration results in two new streams (one lean and the other semilean) with different CO_2 loadings and different $[\text{TAU}/\text{K}]$ ratios. The lean stream has a lower CO_2 loading than the corresponding lean stream in the DECAB Plus baseline configuration. This stream is fed at the top of the absorber column with the aim of increasing the absorption capacity at the top stages of the absorber. The semilean stream has an intermediate CO_2 loading between the lean and rich streams and is fed to an intermediate stage in the absorber column. This configuration also creates a pH gradient within the absorber due to the different $[\text{TAU}/\text{K}]$ ratios. The top stages have a lower pH than the bottom stages.

3.4. Alternative Solvents. Solvent regeneration in the DECAB and DECAB Plus processes relies on the thermal energy provided by the reboiler and the pH-shift effect described in section 2, which helps the reduction of this energy. Both thermal and pH-shift effects in these processes are influenced by specific amino acid properties. For the purpose of selecting a solvent that requires less regeneration energy, there are key solvent characteristics that are of importance, such as the net CO_2 capacity of the solvent, the absorption rates, the heat of absorption, and the heat capacity of the solvent.⁴⁹ The extension of the precipitation reaction during absorption is important to the reduction of the regeneration energy, since the formation of more amino acid precipitates helps to decrease the pH of the new rich stream formed when a fraction of the

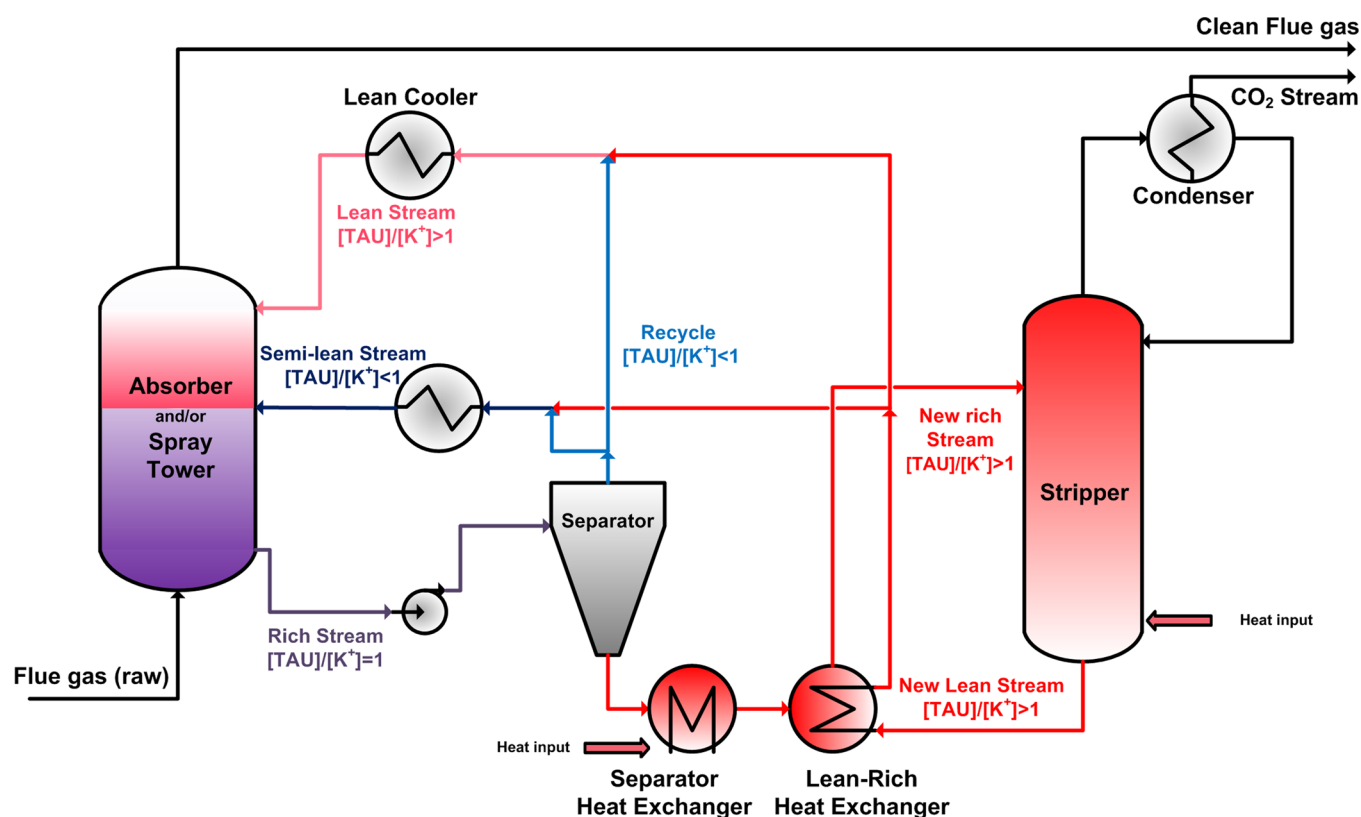


Figure 3. DECAB Plus process based on precipitating potassium taurate with multiple absorber feeds. The process areas with lower pH are highlighted in red. The ratio of the total taurine concentration to the total potassium concentration in solution is indicated below the name of each stream. This ratio can be 1 (equimolar solution), higher than 1 (solution with less potassium than the equimolar solution and, therefore, lower pH_0), or less than 1 (solution with more potassium than the equimolar solution and, therefore, higher pH_0).

Table 1. List of Amino Acids Relevant for Implementation in a DECAB Process Configuration

amino acid	formula	abbreviation	M_w (g/mol)	melting point ⁵¹ (°C)	solubility ⁵¹ (g/100 mL)
taurine	$\text{C}_2\text{H}_7\text{NO}_3\text{S}$	TAU	125	328.0	9.49
α -alanine	$\text{C}_3\text{H}_7\text{NO}_2$	ALA	89	316.5	16.58
2-aminoisobutyric acid (2-methylalanine)	$\text{C}_4\text{H}_9\text{NO}_2$	AIB	103	335.0	12.06–18.40
6-aminohexanoic acid (ϵ -aminocaproic acid)	$\text{C}_6\text{H}_{13}\text{NO}_2$	6-AHA	131	205.0	50.50

supernatant is recycled. The precipitates need to be dissolved for the pH-shift effect to be effective. Therefore, the amino acid solubility, which is relevant to the precipitation, and heat of dissolution, which is relevant to the dissolution of the precipitates, are also important properties for the selection of an alternative solvent for these processes.

With the aim of finding alternative solvents to potassium taurate, the properties of natural amino acids were screened in this work in order to improve process performance. The solvent screening strategy was based on the improvement of the process performance with no-recycle (i.e., no pH-shift effect). The desired amino acid properties for a successful implementation in a DECAB-like process are high capacity for CO_2 , high stability, and relatively higher solubility and lower heat of dissolution than taurine. In order to improve the CO_2 capacity, amino acids with hindered amino groups were targeted, since they generally show higher absorption capacity than primary amino groups.²² Another relevant characteristic is the precipitate type that is formed during the absorption of CO_2 . The more hindered amino acid species tend to form different precipitates than taurine. In some cases, a mixture of amino acid and KHCO_3 is formed,⁵⁰ or in other cases, only KHCO_3 is

formed.⁴³ Although these precipitates are different from the baseline solvent, they are seen as beneficial because they help to increase the net loading (recycling less CO_2 to the absorption column), they will also induce a pH change (the combination of amino acid and HCO_3^- is more acidic than the pure bicarbonate solution), and they offer the possibility of concentrating the rich solution in CO_2 .

Table 1 shows a summary of the amino acids considered most relevant for this application based on these properties. The starting candidates selected were α -alanine or its derivative, 2-methylalanine (2-aminoisobutyric acid), and the 6-aminohexanoic acid. The CO_2 absorption equilibrium isotherms of solutions of the amino acids listed in Table 1 were measured in a well stirred jacketed autoclave at two temperatures (40 and 120 or 130 °C) and concentrations within the precipitation regime of the amino acids. The details of the experimental procedure and results can be found in the Supporting Information to this paper. Absorption mass transfer rates are also important; however, they have not been included at this stage because the models developed for DECAB and DECAB Plus are based on equilibrium. Nevertheless, the relative absorption rates of the solvents with respect to a 30 wt %

Table 2. Empirical Representation of the VL(S)E for the Different Solvents under Investigation (Potassium Taurate [KTAU], Potassium Alanate [KALA], and MEA) and the Corresponding Solvent Vapor Pressures^a

parameter	KTAU VL(S)E, ^b eq 1	KALA VL(S)E, ^c eq 1	MEA VL(S)E, ^d eq 1	KTAU vapor pressure, ^e eq 2	KALA vapor pressure, ^f eq 2	MEA vapor pressure, ^g eq 3
A	-15.44	16.02	42.49	0.47	-1.80	-5.939 × 10 ⁻²
B	9419.69	-6229.32	-17691.20	67.86	99.08	7.621 × 10 ⁻³
C	7.87	10.24	-30.10	-0.45	9.00	-1.90 × 10 ⁻⁴
D	1534.81	0	22210.31	0.00	0.00	2.137 × 10 ⁻⁶
E	1536.86	0	-5531.43	0.00	0.00	0.00
F	64.52	0	0.00	0.00	0.00	0.00
G	3.26	0	0.00	0.00	0.00	0.00
H	-1561.5	0	0.00	0.00	0.00	0.00
Regression Results						
multiple R	0.984	0.986	0.989	0.989	0.985	0.986
standard error	0.322	0.378	0.476	0.04	0.06	0.05
number of observations	118	28	112	179	227	300
SSE ^h	24900	2633	7.94 × 10 ⁷	0.06	0.08	0.07
ARD% ⁱ	24.8%	27%	41%	3%	5%	3%

^aThe coefficients in eqs 1, 2, and 3 are obtained by multiple linear regression, which requires the linearization of the equations. ^bDerived for potassium taurate solutions with [TAU/K] from 1 to 1.3 and temperatures from 40 to 130 °C. ^cDerived for potassium alanate solutions, equimolar, and temperatures of 40 and 120 °C (this work). ^dDerived for 30 wt % MEA based on the data from Lee⁵² and Shen and Li.⁵³ ^eDerived for potassium taurate solutions with concentrations from 2 to 6 M. ^fDerived for potassium alanate solutions with concentrations from 2 to 6 M (this work). ^gDerived for MEA solutions of 30 wt %. ^hSSE: sum of squared errors between the experimental and model values. ⁱARD%: averaged relative deviation between the experimental and model values. ^jEquations:

$$\ln(p^{\text{CO}_2^{\text{eq}}}) = A + \frac{B}{T} + C \cdot \alpha + D \cdot \frac{\alpha}{T} + E \cdot \frac{\alpha^2}{T} + F \cdot \frac{\ln(\alpha)}{T} + G \cdot \text{pH}_0 + H \cdot \frac{\text{pH}_0}{T} \quad (1)$$

$$p^{\text{H}_2\text{O}} = \left(1 - \left(A + \frac{B \cdot X_s}{T} + C \cdot x_s \right) \cdot x_s \right) \cdot p^{\text{H}_2\text{O}^0} \quad (2)$$

$$p^{\text{H}_2\text{O}} = A + B \cdot T + C \cdot T^2 + D \cdot T^3 \quad (3)$$

$p^{\text{CO}_2^{\text{eq}}}$ is the equilibrium CO₂ partial pressure (kPa), $p^{\text{H}_2\text{O}}$ is the vapor pressure of the solutions (bar), $p^{\text{H}_2\text{O}^0}$ is the pure water vapor pressure (bar), a is the CO₂ loading (mol of CO₂/mol of AmA), T is the temperature (°C), pH_0 is the initial pH of the solution, and x_s is the total mole fraction of amino acids and potassium in solution.

MEA solution were inspected during the absorption experiments by comparing the time to reach equilibrium of the different solvents and MEA. This procedure was used to rule out solvents with substantially lower absorption rates than MEA. The precipitates formed during absorption were analyzed by the phosphoric acid method in order to determine the presence of carbonates in the precipitates. The experimental procedure is described in the Supporting Information.

4. MODEL DEVELOPMENT

An equilibrium process model (VLEMS) has been developed for aqueous solutions of amino acids and MEA and has been used for the evaluation of the different process configurations proposed in this work. The absorption and desorption performances are estimated by a series of equilibrium stages where the mass balances, enthalpy balance, and equilibrium relations are simultaneously solved, providing the temperature and composition profiles and the reboiler energy. The model is based on the following assumptions:

- The only components that are considered in the VLE calculations are CO₂ and water. Amino acids are non-

volatile, and in the case of amines, the vaporization is neglected.

- Each stage is assumed to be well mixed, and process conditions and gas and liquid composition are uniform in each stage.
- Temperature, pressure, and material equilibrium are reached in each stage.
- The reboiler is considered as an equilibrium stage
- Heat losses are not considered.

The vapor–liquid–solid equilibrium (VL(S)E) data for the amino acid salts under investigation are necessary to estimate solid–liquid partition and vapor–liquid equilibrium (VLE) under different conditions. In our previous work,⁴⁷ a conceptual design methodology was introduced, which required three different experimental tests: the pH determination of solutions containing different concentrations of amino acid and potassium hydroxide, the measurement of the VLE on those solutions at different temperatures, and the determination of the weight of solids and solid type formed during CO₂ absorption in those solutions. The results of each experiment were fitted to empirical expressions that provided the estimation of the VL(S)E under different conditions.⁴⁷

Table 2 shows the empirical expressions used to estimate the VL(S)E of CO₂ in 4 M potassium taurate,⁴⁷ 4 M potassium alanate (measured in this work), and MEA (from literature data^{52,53}) solutions and the correlations to estimate the water vapor pressure of these solutions under different conditions. In the equilibrium model, a constant value of 0.8 Murphree efficiency is applied at every stage for CO₂. This value was selected to fit the experimental results of Knudsen⁵⁴ for MEA, which were conducted at the pilot plant of Dong at the Esbjerg power plant station. For the other solvents (potassium taurate and alanate), the same value of the Murphree efficiency was used due to the lack of pilot plant experimental results with these solvents. This assumption is equivalent to assuming similar absorption rates to MEA for these two solvents and could lead to loadings that deviate from those attainable under real operating conditions. Although this could be a limiting factor for future process implementation, it was considered acceptable for the conceptual design because the objective is to screen multiple solvents and process configurations. The model assumptions could be checked in future studies for an optimal solvent and process configuration. The heat of absorption/desorption of CO₂ is calculated by differentiating eq 1 in footnote *j* of Table 2 with respect to 1/*T*. The heat of vaporization of water and the heat capacity of steam are calculated with the equations from the Steam Tables of the IAPWS-IF97 industrial standard.⁵⁵ The molar gas heat capacity for CO₂ is calculated with equations from the NIST database.⁵⁶ In the case of liquid enthalpy calculation, the overall heat capacity of the entire solution is used. A representative constant value has been used for taurine⁵⁷ and alanine.⁵⁸ This method neglects the addition of CO₂ to the liquid. Solvent density is considered equal for all trays and given a representative constant value which has been derived from the literature.⁵⁸

A number of process variables are important to the evaluation of the DECAB and DECAB Plus process concepts:

- Taurine-to-potassium molar ratio ([TAU/K]): Represents the ratio of the total concentration of taurine to the total concentration of potassium, which is equal to the concentration of KOH used to prepared the amino acid salt solution.
- Initial pH of taurine–KOH solutions (pH₀): Represents the pH of an aqueous solution of taurine and KOH measured at 40 °C. It is related to [TAU/K], as shown in our previous work:⁴⁷

$$\text{pH}_0 = f\left(\frac{[\text{TAU}]}{[\text{K}^+]}\right) \quad (4)$$

- Recycle split fraction (RSF): Represents the fraction of the liquid supernatant (excluding the solid phase) that is recycled to the absorber column.

$$\text{RSF} = \frac{L_R}{L - S} \quad (5)$$

Here, *L_R* represents the flow (kmol/s) of the recycle stream, *L* represents the flow (kmol/s) of the total rich stream leaving the absorber, and *S* represents the flow (kmol/s) of the solid phase.

- Specific regeneration energy: The energy necessary for regeneration, calculated by the process model considering the reboiler duty and the energy required to power the compressor, in the cases where the LVC is applied.

An isentropic efficiency of 88% and a driver efficiency of 85% are assumed in the calculations of compressor power. The results are presented as steam equivalent (GJ/tCO₂) energy that will result in the same turbine power loss as deducting the compressor power from the gross turbine power output, according to the formula

$$Q_t = Q_R + \frac{W_{\text{COMP}}}{\lambda} \quad (6)$$

In the equation above, *Q_t* is the total specific regeneration energy, *Q_R* is the estimated reboiler duty for solvent regeneration, and *W_{COMP}* is the estimated work for the LVC compressor. The term *λ* accounts for the loss of turbine power due to steam extraction for the reboiler. This factor depends on the necessary steam quality and is derived for each case from the power plant and capture plant integration correlations developed by Le Moulec.³⁵ Equation 6 should only be used to compare cases where the steam quality is similar.

- Total power plant parasitic load: The integration of DECAB and DECAB Plus into coal fired power plants requires the use of two different energy sources. On one hand, the reboiler needs saturated steam at pressures between 3 and 4 bar, depending on the reboiler conditions. On the other hand, the separator requires low grade energy for the dissolution of crystals. In this case, steam of very low pressure (ca. 1 bar) has been used in order to provide the necessary energy required by the separator heat exchanger. The model developed by Le Moulec³⁵ was used to calculate the parasitic load to a hypothetical power plant with implemented capture based on DECAB and DECAB Plus.

$$W_t = W_R + W_{\text{LVC}} + W_{\text{SEP}} + W_{\text{COMP}} \quad (7)$$

Here, *W_t* (kWh/tCO₂) is the total power plant parasitic load, *W_R* (kWh/tCO₂) is the equivalent work needed for the reboiler, *W_{LVC}* (kWh/tCO₂) is the energy required by the LVC compressor, *W_{SEP}* (kWh/tCO₂) is the equivalent work required by the separator, and *W_{COMP}* (kWh/tCO₂) is the energy required to compress the CO₂ from the pressure at the top of the stripper to 110 bar.

5. RESULTS AND DISCUSSION

5.1. Baseline Case Optimization. The optimization of the lean loading without any recycle (DECAB configuration) at different reboiler temperatures is shown in Figure 4. The minimum specific reboiler duty occurs at a CO₂ loading of 0.26–0.27 mol of CO₂/mol of TAU for every temperature. The effect of the reboiler operating temperature is not very substantial but is appreciable from the results in Figure 4. Higher reboiler temperatures lead to lower specific reboiler duties due to a more favorable water to CO₂ ratio at the stripper's top stage conditions. For every temperature analyzed in Figure 4, the reboiler pressure was fixed at the value that provides the optimum lean loading. Subsequently, the recycle split fraction (RSF) was varied from 0 to 50% in order to induce the pH-shift effect of the DECAB Plus process configuration. This broad range was selected in order to study the influence of the pH-shift effect in a broad operating range. The results of the slurry tests in our previous work⁴⁷ indicate that the [TAU/K] ratio should be restricted to a range

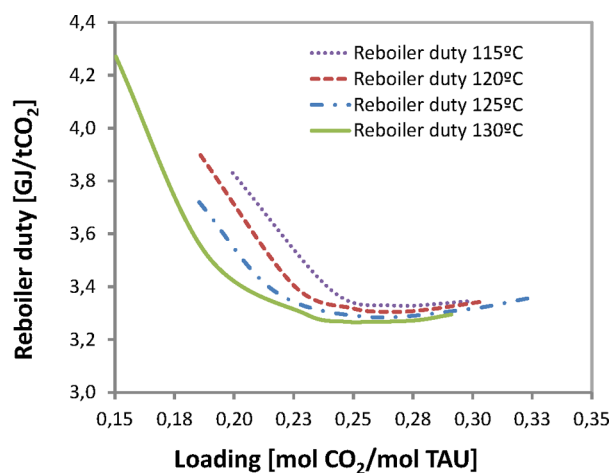


Figure 4. Optimization of specific reboiler duty with respect to reboiler temperature for potassium taurate and the DECAB process configuration illustrated in Figure 1. Simulations were performed at a constant recycle split fraction (RSF) of 0% and constant CO₂ removal of 90%.

from 1 to 1.2 to avoid the presence of any solids in the new rich stream fed to the stripper. The values of the RSF above 40% fall outside this range; however, they have been included in the simulations in order to develop a full understanding of the pH-shift effect. Figure 5 shows the optimization of the RSF at

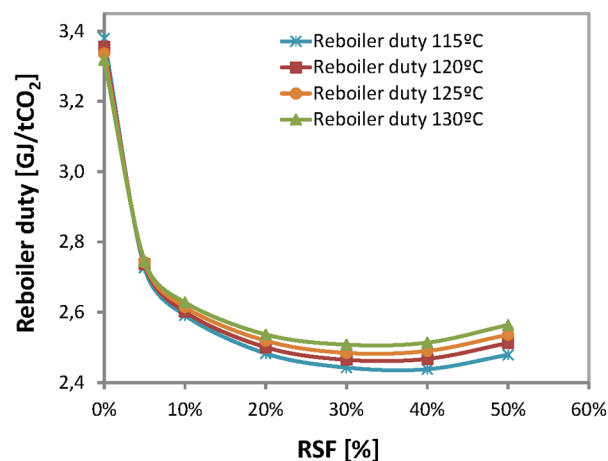


Figure 5. Optimization of the reboiler duty with respect to the recycle split fraction (RSF) at different temperatures for the DECAB Plus process configuration illustrated in Figure 1. Simulations were performed at the optimum lean loading for every temperature and a constant CO₂ removal of 90%.

different reboiler temperatures. The DECAB Plus process configuration reduces the specific reboiler energy by 27–29% depending on the operating reboiler temperature. For all temperatures, the value of the RSF that minimizes the specific reboiler duty is around 30%. For higher values of the RSF, the net capacity of the solvent is considerably reduced due to the recycle of the absorbed CO₂ back to the absorber column. For these cases, the solvent flow needs to be increased substantially, to maintain the CO₂ removal percentage at 90%, leading to an increase in the required reboiler duty. For the DECAB Plus configuration, lower reboiler temperatures lead to lower specific reboiler duties, despite the fact that for the DECAB configuration (i.e., 0% RSF) the opposite behavior was found.

This change can be explained by the variation of the pH-shift effect with temperature. Figure 6 shows the influence of pH₀ on

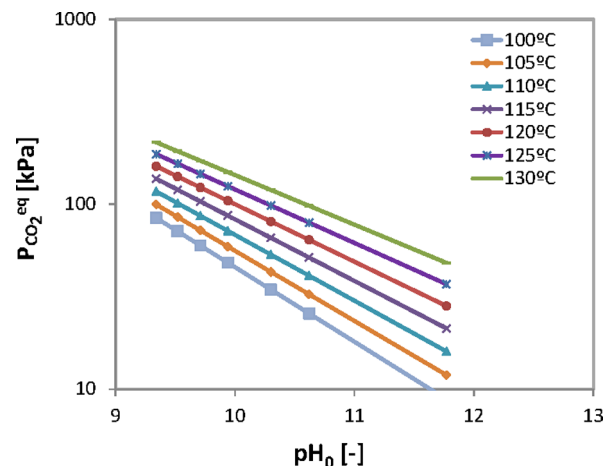


Figure 6. Influence of pH₀ on the equilibrium partial pressure of CO₂. Simulations were performed at a constant loading, corresponding to the optimum lean loading.

the equilibrium partial pressure of CO₂ at optimum lean loading conditions. When the pH₀ is decreased, the equilibrium partial pressure of CO₂ increases significantly. However, for higher values of temperatures, the effect becomes less prominent, as indicated by the reduction in the slope of the P^{CO₂} vs pH₀ lines represented in Figure 6. Therefore, the RSF has a more marked effect on the reboiler duty at lower temperatures than at higher temperatures.

For further optimization of the DECAB Plus process, the reboiler temperature and the RSF were fixed and the separator temperature was decreased from 40 to 25 °C. The implications for the process are the precipitation of more solids, the need of extra cooling duty in the separator, and the increase in the specific energy required to re-dissolve the precipitates. This modification results in higher [TAU/K] in the new rich stream for equal values of the RSF. Figure 7 shows the results for a reboiler temperature of 120 °C and 20% RSF. Although the

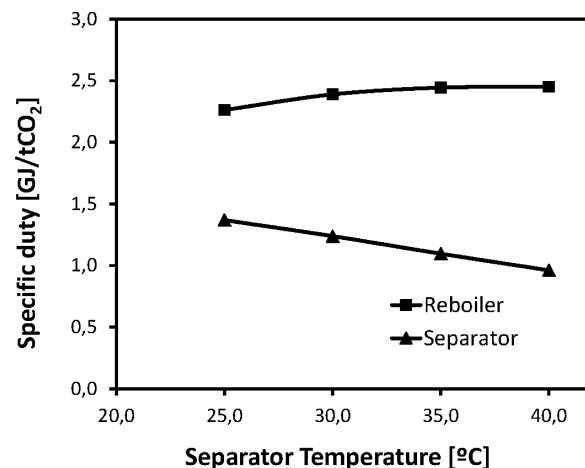


Figure 7. Variation of the reboiler and separator duties with the separator operating temperature for the DECAB Plus process concept illustrated in Figure 1. Simulations are done at fixed reboiler temperature (120 °C), 20% recycle split fraction (RSF), and a constant CO₂ removal of 90%.

optimal value found for this variable is 30% (Figure 5), the reduction in the reboiler duty when the RSF increases from 20 to 30% is not significant and it will imply the processing of a more dense slurry and a larger recycle stream (with implications to the sizing of the absorption process). Decreasing the separator operating temperature results in lower reboiler duties due to the extra pH-shift effect induced by a higher [TAU/K] ratio in the new rich stream. However, as indicated in Figure 7, this also increases the specific separator energy.

5.2. Lean Vapor Compression (LVC). For the evaluation of the LVC addition to the DECAB and DECAB Plus concepts, several simulations were performed at different reboiler temperatures. The reboiler pressure was kept constant at the value that minimized the specific reboiler duty for every temperature. The pressure in the flash vessel was decreased gradually, starting from a value equal to the reboiler pressure, to atmospheric conditions. The results of these simulations are shown in Figure 8 for reboiler temperatures of 120 and 130 °C.

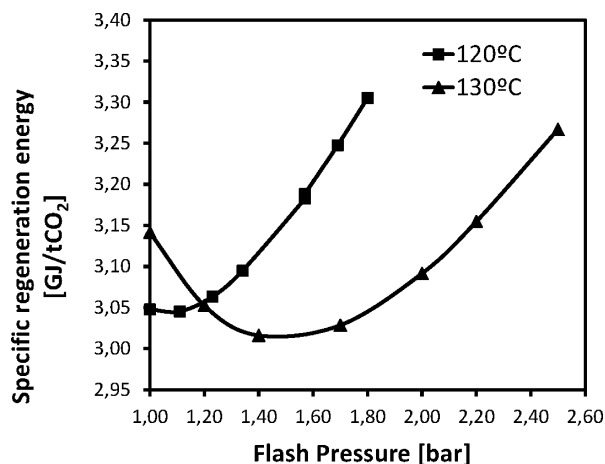


Figure 8. Optimization of LVC flash pressure for the DECAB process concept with LVC illustrated in Figure 2. Simulations were performed at constant reboiler pressure corresponding to the optimal value for every temperature, no recycle split fraction (0% RSF), and a constant CO₂ removal of 90%.

Figure 8 shows the specific energy requirements of the reboiler, which include the energy required to power the compressor in the form of steam that would result in a power loss to the turbine equivalent to the LVC compressor power. When the rich stream is flashed, the reboiler duty necessary to regenerate the solvent is reduced due to the extra steam generated. The extra steam is then compressed to the reboiler pressure and fed back to the stripper. As shown in Figure 8, the total energy required for regeneration decreases with decreasing flash pressures. However, for flash pressures near atmospheric conditions, the energy required by the compressor becomes a dominant contributor to the total energy requirements and, therefore, the specific energy requirements raise. At 120 °C, a pressure difference between the reboiler and the flash vessel of 0.69 bar provides a minimum in the total energy required. At 130 °C, the minimum is reached at a pressure difference of 1.10 bar. The reductions in the specific energy requirements are 7.9 and 7.7% for 120 and 130 °C, respectively. However, operating the reboiler at 130 °C requires condensing steam of higher pressure than at 120 °C. The implications of changing the steam quality are further discussed in section 5.5.

The influence of LVC on the DECAB Plus process configuration was also investigated at constant reboiler temperatures and pressures. Figure 9 shows the influence of

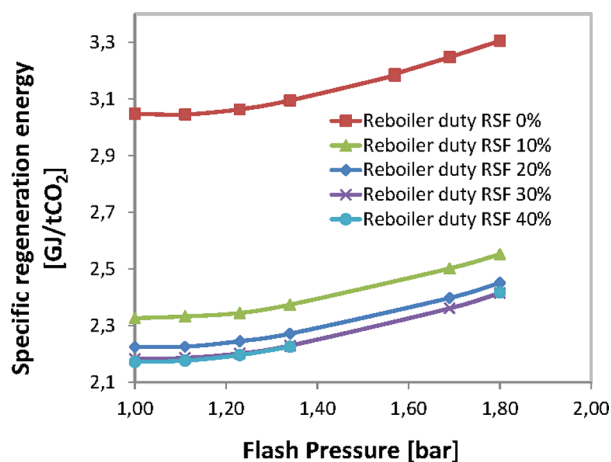


Figure 9. Effect of LVC flash pressure on the specific regeneration energy for the DECAB Plus process concept with LVC illustrated in Figure 2. Simulations were performed at constant reboiler temperature (120 °C), different values of the recycle split fraction (0–40% RSF), and a constant CO₂ removal of 90%.

the LVC flash pressure on the specific regeneration energy at 120 °C and different values of the RSF. The effect of flashing the lean stream on the total energy required to regenerate the solvent is similar for every value of the RSF. In relative terms, the value of the initial specific energy is reduced from 7.9 to 10.0% when the RSF increases from 0 to 40%.

5.3. Multiple Absorber Feeds. This process configuration is most appropriated for the cases with a high RSF (above 30%) where the recycle of the absorbed CO₂ back to the absorber column reduces considerably the net capacity of the solvent (see section 5.1). The configuration aims, a priori, to increase solvent capacity by using a stream at the top of the absorber of a lower CO₂ loading. For this purpose, the recycle and the new lean stream leaving the stripper are split in two. One fraction of the recycle stream is mixed with the major fraction of the new lean stream from the stripper and sent to the top of the absorber (Figure 3). The remaining fraction of the recycle stream is fed at an intermediate stage of the absorber together with the remaining fraction of the new lean stream (if there is one). The effect of this configuration on the required reboiler duty is shown in Figure 10. For this case, the RSF was fixed at 30%, which is a relatively high value at which the net capacity of the solvent starts to decline. The new lean stream was entirely sent to the top of the absorber, and the fraction of the recycle stream that is mixed with it was gradually decreased from 100% (all the recycle stream is mixed with the new lean stream, resulting in a [TAU/K] of 1) to 80% (only 80% of the recycle stream is mixed with the new lean stream, resulting in a [TAU/K] higher than 1). By splitting the recycle stream, the pH₀ in the lean stream decreases from 11.77 (value that corresponds to the equimolar solution, [TAU/K] = 1.00) to 10.54 (value that corresponds to [TAU/K] = 1.02). The loading of the lean stream also decreases from 0.29 mol of CO₂/mol of TAU to 0.26 mol of CO₂/mol of TAU. However, this modification does not have a positive effect on the reboiler duty, which increases gradually. This is due to the effect that pH has on the equilibrium absorption of CO₂. The equilibrium partial

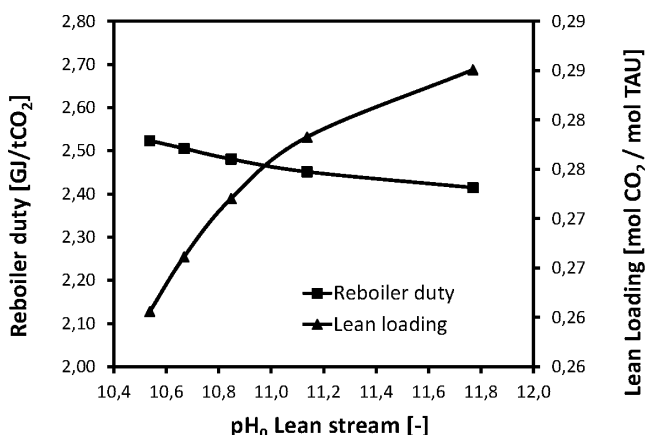


Figure 10. Effect of multiple absorber feeds on the DECAB Plus process concept illustrated in Figure 3. Lean stream loading and reboiler duty vs pH_0 in the lean stream. Simulations were performed at a constant reboiler temperature ($120\text{ }^\circ\text{C}$) and a constant CO_2 removal of 90%.

pressure of CO_2 at the top of the absorber increases with lower pH_0 and decreases with lower CO_2 loadings. The reduction in the pH_0 of the lean stream has a substantial impact on the reboiler duty due to the reduction in solvent capacity, which is not compensated by the reduction in lean loading obtained in this process configuration. Therefore, the multiple absorber feeds configuration leads to a higher reboiler duty than in the other process configurations. For this reason, this alternative was discarded for further evaluation.

5.4. Alternative Solvents. The absorption capacity of a selected number of amino acids was investigated at 40 and $120\text{ }^\circ\text{C}$ or $130\text{ }^\circ\text{C}$ and compared to potassium taurate. Figure 11 shows the isotherms for the absorption of CO_2 in these solvents. The majority of the solutions tested showed higher absorption capacity (on a mol-to-mol basis) than potassium taurate at partial pressures of CO_2 relevant for flue gas application (ca. 10 kPa). With respect to regeneration, the 6-aminohexanoic acid solution (6-AHA) showed a lower partial pressures of CO_2 than taurine at $120\text{ }^\circ\text{C}$, which implies that more stripping steam will be required to regenerate this solvent with the consequent impact on the thermal regeneration energy. The 4 M 2-aminoisobutyric acid (AIB) solution required a temperature of $130\text{ }^\circ\text{C}$ in order to obtain a similar isotherm to the other amino acids at $120\text{ }^\circ\text{C}$. The low CO_2 partial pressures obtained initially at $120\text{ }^\circ\text{C}$ indicated that this temperature was not suitable for an effective regeneration of this solution. Raising the temperature to $130\text{ }^\circ\text{C}$ was not required when the AIB concentration was reduced to 2 M, but this reduces the bulk capacity of the solution.

The critical points for solvent precipitation were determined by visual inspection of the samples during CO_2 absorption. These points are shown in Figure 11 by empty markers. In the 6-AHA sample, precipitates were formed at relatively high liquid loadings of 0.6 mol of CO_2 /mol of AmA. This is to be expected, since this amino acid is more soluble than the other amino acids tested. However, in the case of α -alanine and 4 M AIB, precipitation occurred at lower loadings than taurine, 0.26 and 0.15 mol of CO_2 /mol of AmA, respectively, despite these two amino acids being more soluble. Decreasing the concentration of AIB from 4 to 2 M shifted the precipitation point to 0.64 mol of CO_2 /mol of AmA. These results have an effect on the application of these solutions to the DECAB and

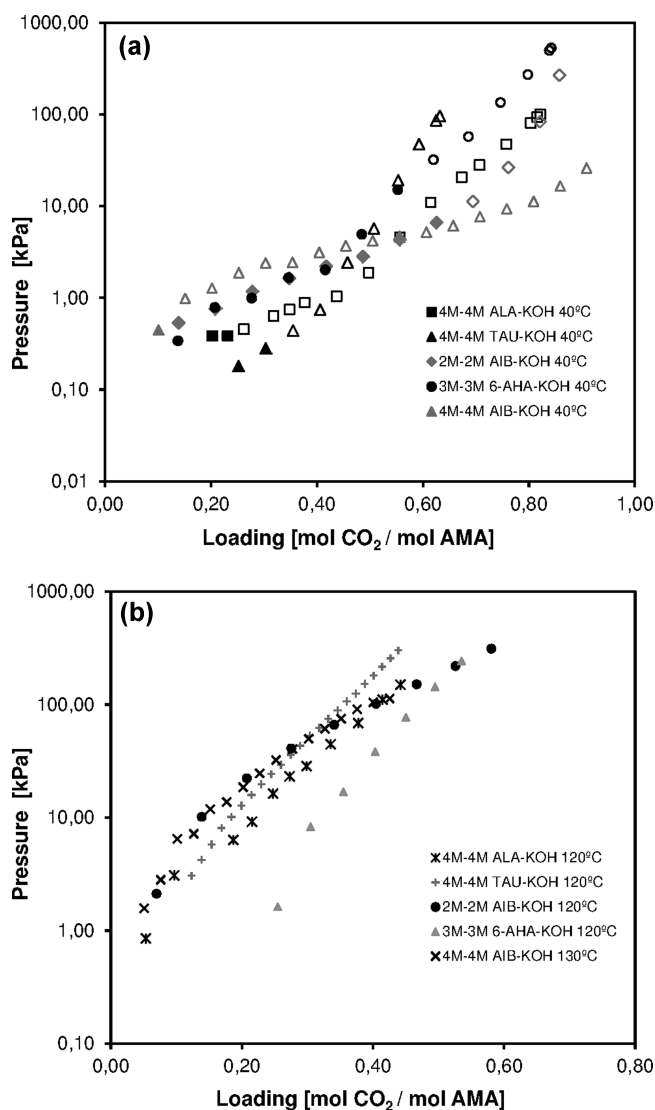


Figure 11. Absorption equilibrium of CO_2 (VLE) in aqueous amino acid solutions at different temperatures measured in this work. The legend indicates the total concentrations of amino acid and potassium hydroxide (KOH) in solution. The empty markers indicate the presence of solids in the liquid phase at equilibrium.

DECAB Plus processes. In the 6-AHA solution, precipitates are formed at a high CO_2 partial pressure, which decreases the enhancement effect during absorption. On the other hand, in the 4 M AIB solution, precipitates are formed at very low CO_2 partial pressures, which will require a deep regeneration to keep the lean loading below the critical point for precipitation. This issue can be solved by reducing the AIB concentration, but this will also reduce the bulk CO_2 capacity of the solution.

Considering the absorption and precipitation characteristics, the most promising amino acid tested is α -alanine. The potassium alanate solution tested had higher specific capacity than taurine and a similar regeneration isotherm. Other attractive properties of α -alanine for its application in DECAB and DECAB Plus processes are higher solubility than taurine and much lower dissolution energy.^{59,60} Therefore, this amino acid was included in the process model in order to evaluate its performance in a DECAB configuration.

The DECAB process based on 4 M potassium alanate is essentially the same as the one for potassium taurate, which has

been described in section 2. For process evaluation, the absorption data of CO₂ on potassium alanate and the vapor pressure data of the potassium alanate solution were fitted to eqs 1 and 2 in footnote *j* of Table 2, respectively. The empirical correlations presented in this table were used to describe the VLE of this solvent.

The precipitation characteristics of potassium alanate were further investigated by analyzing the precipitates formed using titration to determine the amino acid concentration and phosphoric acid analysis to determine the presence of bicarbonates in the precipitate. The potassium salt of α -alanine solution formed a slurry containing 21 wt % (dry) solids of which 13 wt % (dry) were bicarbonate species. The analysis procedure and experimental data are provided in the Supporting Information. The other necessary physical properties were retrieved from the literature as explained in section 4.

For a DECAB configuration basis, the optimization of the lean loading for potassium alanate at different reboiler temperatures is shown in Figure 12. The minimum specific

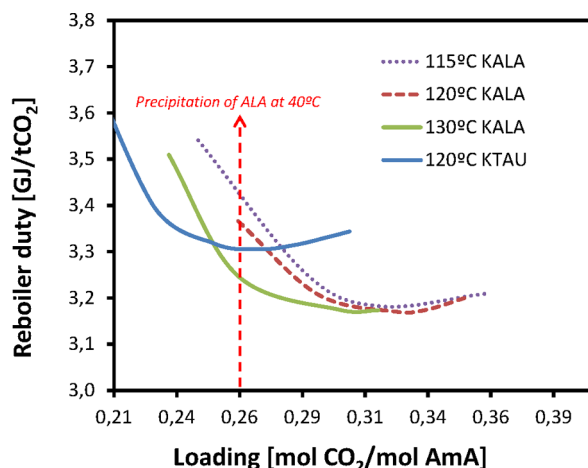


Figure 12. Optimization of specific reboiler duty with respect to reboiler temperature for potassium alanate and the DECAB process configuration illustrated in Figure 1. Simulations were performed at a constant recycle split fraction (RSF) of 0% and constant CO₂ removal of 90%.

reboiler duty occurs at a CO₂ loading of 0.32–0.33 mol of CO₂/mol of ALA. At this loading, the specific reboiler duty for potassium alanate is lower than that for potassium taurate (also included in the figure). Nevertheless, for loadings above 0.26 mol of CO₂/mol of ALA, precipitates will form at temperatures around 40 °C. Therefore, the loading needs to be restricted at that value to avoid precipitation of the lean stream when it is fed to the absorber. The minimum reboiler duty is then 3.25 GJ/tCO₂, with a reboiler temperature of 130 °C. With the addition of LVC to the process, the specific regeneration energy can be reduced to 2.81 GJ/tCO₂.

5.5. Evaluation of Process Alternatives. This section provides an overview of the process concepts analyzed in this work and their performances. Table 3 shows the performance of the process configurations investigated and the most optimal process conditions of each configuration. The evaluation of a conventional 30 wt % MEA capture process, based on the same model and assumptions as in the other process configurations, has been added to the table for comparison. The evaluation is based on the equivalent work of each configuration, which has been calculated with the model developed by Le Moullec³⁵ and

includes the energy use of each process configuration, the work of the LVC compressor (when present), and the work to compress the CO₂ to 110 bar. This model focuses on retrofitting a coal fired supercritical power plant of 1200MWe gross with re-superheating of the intermediate pressure steam. The steam for the boiler is drawn off between the IP and LP turbines at 5.9 bar, is expanded through an auxiliary turbine to reduce the pressure to the optimum working pressure in the reboiler, and then is cooled by preheating the power plant boiler working water before being fed to the capture plant reboiler. The reboiler condensate energy (at around 135 °C) is also used in the preheating train of working water. A similar scheme could be used for the separator, assuming that the IP/LP turbine line has enough steam flow to supply the reboiler and separator and to operate the low pressure turbine. Before entering the turbine, the pressure of the working steam is increased proportionally to the drawn off flow rate using a throttle valve. In this way, the different qualities of steam required by the separator and the reboiler and the electricity supply for the compressors are considered. The consumption of the CO₂ compressor (used to deliver the CO₂ at a pressure of 110 bar) is also calculated with this model, considering the differences in the delivery pressure of the CO₂ stream from the stripper.

The lean loading of the MEA and TAU process configurations was optimized to minimize the reboiler duty. In the case of alanine (ALA), the maximum lean loading was fixed at 0.26 mol of CO₂/mol of ALA, because precipitates will form in the lean stream at 40 °C and higher loadings. This loading is far from the optimum. Therefore, the reduction in the overall energy required by the DECAB process when the solvent is changed from taurine to alanine is not substantial. The major savings with respect to taurine rely on the lower heat of dissolution of alanine, resulting in lower energy required by the separator to dissolve the precipitates.

The optimization of operating conditions was based on the reduction of reboiler energy. On the basis of potassium taurate, the DECAB process configuration reduces the reboiler duty but at the expense of increasing the separator energy. Under the integration conditions suggested by Le Moullec,³⁵ which might not be optimal for the integration of the separator energy into the steam cycle, there is no real gain in the overall energy use of the DECAB configuration as compared to conventional MEA.

The addition of the LVC to the process reduces the overall energy requirements of the DECAB process configuration. In the case of potassium alanate, the required energy is lower than the MEA baseline with savings of 6%, which is similar to the savings obtained by adding the LVC to the MEA conventional process configuration. Nevertheless, the DECAB Plus configuration has a net beneficial impact on the energy use of the capture process. However, the reduction of the reboiler duty by RSF values over 20% or by reducing the separator temperature to room temperature does not result in a reduction of the overall energy required by the capture process. The best configuration is the DECAB Plus with LVC, which provides 15% energy savings with respect to MEA and 8.5% with respect to MEA with LVC.

6. CONCLUSIONS

DECAB and DECAB Plus are two novel process concepts based on precipitating amino acids that can reduce the regeneration energy required by the CO₂ capture process. An analysis of process conditions and different configurations of

Table 3. Predicted Performance of Various Solvents and Process Configurations for 90% CO₂ Capture from Flue Gas Originating from a Coal Fired Power Plant^a

process configuration	solvent	reboiler			S–L separator ^c		LVC	energy			work			
		<i>T</i> (°C)	<i>P</i> (bar)	<i>P_s</i> (bar)	<i>T</i> (°C)	RSF (%)	<i>P</i> (bar)	<i>Q_R</i> (GJ/t)	<i>Q_{SEP}</i> (GJ/t)	<i>W_R</i> (kWh/t)	<i>W_{LVC}</i> (kWh/t)	<i>W_{SEP}</i> (kWh/t)	<i>W_{COMP}</i> (kWh/t)	<i>W_T</i> (kWh/t)
conventional	MEA ^b	120	1.9	3.13	NA	NA	1.9	3.66	0.00	309.8	0.0	0.0	93.6	403.4
conventional + LVC	MEA	120	1.9	3.13	NA	NA	1.2	3.18	0.00	272.7	9.2	0.0	93.6	375.5
DECAB	TAU	120	1.8	3.13	40	0%	1.8	3.31	1.01	282.7	0.0	63.4	95.2	441.3
DECAB	ALA	120	1.8	3.13	40	0%	1.8	3.37	0.56	287.4	0.0	35.4	95.2	418.0
DECAB	ALA	130	2.5	4.16	0	0%	2.5	3.20	0.55	301.4	0.0	34.7	85.4	421.5
DECAB + LVC	TAU	120	1.8	3.13	40	0%	1.1	2.86	0.93	247.5	12.1	58.3	95.2	413.1
DECAB + LVC	ALA	130	2.6	4.16	40	0%	1.4	2.52	0.54	242.1	18.2	34.5	84.2	379.1
DECAB Plus	TAU	120	1.8	3.13	40	20%	1.8	2.45	0.96	214.8	0.0	60.2	95.2	370.2
DECAB Plus	TAU	115	1.5	2.70	40	40%	1.8	2.39	1.24	199.7	0.0	77.0	100.7	377.4
DECAB Plus	TAU	120	1.8	3.13	25	20%	1.8	2.26	1.37	199.3	0.0	84.8	95.2	379.3
DECAB Plus + LVC	TAU	120	1.8	3.13	40	20%	1.1	2.07	0.88	183.5	9.9	55.1	95.2	343.6
DECAB Plus + LVC	TAU	120	1.8	3.13	25	20%	1.1	1.90	1.24	169.1	9.7	77.4	95.2	351.4

^aThe working conditions of the reboiler and the solid–liquid (S–L) separator are provided: temperature (*T*), pressure (*P*), and the pressure of condensing steam required (*P_s*). ^bOn the basis of the results of Sanchez Fernandez et al.⁴⁷ ^cThe steam pressure (*P_s*) is 1 bar in all cases.

these two process concepts has been conducted on the basis of the necessary energy to regenerate the solvent. The configurations analyzed contribute to decrease this energy with the only exception of the multiple feeds to the absorber. This configuration was aimed to increase the solvent capacity by using a lean stream at the top of the absorber column with lower loading than the DECAB Plus baseline configuration. However, the lower pH of this stream did not decrease the regeneration energy as expected.

The developed process configurations also require low-grade energy to dissolve the precipitates formed during absorption. The energy requirements of the reboiler and the separator heat exchanger were added to calculate the overall energy requirements of the process. The DECAB process configuration based on taurine reduces the reboiler energy by 10% with respect to conventional MEA and by 12% when LVC is added. However, this reduction is accompanied by an increase in the energy required by the separator heat exchanger to dissolve the precipitates. Under the assumptions considered for the retrofit of these processes into power plants, which are based on a pre-existing model and are not optimal for the integration of the separator energy into the steam cycle, the final energy use of these process alternatives is higher than the conventional MEA process. Nevertheless, all the DECAB Plus configurations analyzed reduce the overall energy use of the capture process with respect to the MEA baseline. The best process configuration in this study is the DECAB Plus process configuration based on potassium taurate with a reboiler temperature of 120 °C and solid–liquid separation at 40 °C. This alternative reduces the overall energy of the capture process by 15% compared to the MEA baseline with compression of the CO₂ to 110 bar.

Other amino acid solvents were investigated in this work in order to explore potential reductions in the energy required by the DECAB process configuration. Among the solvents investigated, the potassium salt of α -alanine was identified as a potential candidate for the application in the DECAB configuration. The performance of the DECAB configuration based on potassium alanate is better than potassium taurate due

to the lower heat of dissolution of α -alanine. With the addition of LVC, it reduces the energy penalty of the MEA baseline by 6%. Considering the benefits that the DECAB configuration with potassium alanate has over potassium taurate, a DECAB Plus configuration based on this solvent has the potential to further reduce the energy requirements of the capture process. Moreover, a better integration within the steam cycle should reduce the energy figures presented in this work.

■ ASSOCIATED CONTENT

📄 Supporting Information

The experimental data graphically presented in Figure 11 is tabulated with detailed experimental conditions. The experimental procedures to determine the amount of precipitates formed in potassium alanate solutions are also provided. This material is available free of charge via the Internet at <http://pubs.acs.org>.

■ AUTHOR INFORMATION

Corresponding Author

*E-mail: eva.sanchez@processmonkey.co.uk.

Notes

The authors declare no competing financial interest.

■ ACKNOWLEDGMENTS

The authors would like to thank the CATO-2 program and its sponsors for financing this research.

■ NOTATION

- 6-AHA 6-aminohexanoic acid
- AIB 2-aminoisobutyric acid
- ALA α -alanine
- AMA amino acid (represents the zwitterion species)
- AMAK⁺ potassium salt of an amino acid (represents the species that has the amine group deprotonated)
- ARD% average relative deviation
- LVC lean vapor compression
- KALA potassium alanate
- KTAU potassium taurate

RSF recycle split fraction (%)
 SSE sum of squared errors
 TAU total amount of taurine species (mol)
 VLEMS vapor–liquid equilibrium multistage model

Symbols

P pressure (bar)
 pH_0 pH of a solution containing taurine and KOH (-)
 P_{CO_2} equilibrium partial pressure of CO₂ (kPa)
 P_s steam pressure (bar)
 Q specific thermal energy requirement (GJ/tCO₂)
 T temperature (°C)
 W specific work requirement (kWh/tCO₂)

Greek Symbols

α liquid CO₂ loading (mol of CO₂/mol of AMA)

Subindexes

t total
 R reboiler
 LVC LVC compressor
 SEP separator
 COMP CO₂ compressor

REFERENCES

- (1) EEA. *Air Pollution Impacts from Carbon Capture and Storage (CCS)*; European Environmental Agency technical report No 14. Copenhagen, 2011. Available at <http://www.eea.europa.eu/>.
- (2) IEA. *CO₂ Capture and Storage -- A Key Carbon Abatement Option*; International Energy Agency: Paris, 2008; ISBN 978-92-64-041400.
- (3) IPCC. *Climate Change 2007: Mitigation, Contribution of Working Group III to the Fourth Assessment Report of the Intergovernmental Panel on Climate Change*; Cambridge University Press: Cambridge, U.K., 2007.
- (4) Herzog, H. J. Scaling up carbon dioxide capture and storage: From megatons to gigatons. *Energy Econ.* **2011**, *33* (4), 597–604.
- (5) Davison, J. Performance and costs of power plants with capture and storage of CO₂. *Energy* **2007**, *32* (7), 1163–1176.
- (6) Gibbins, J. R.; Crane, R. I. Scope for reductions in the cost of CO₂ capture using flue gas scrubbing with amine solvents. *Proc. Inst. Mech. Eng., Part A* **2004**, *218* (4), 231–239.
- (7) Finkenrath, M. Cost performance of carbon dioxide capture from power generation. *International Energy Agency* 2010, OECD/IEA: Paris.
- (8) Oexmann, J.; Kather, A. Post-Combustion CO₂-Capture from Coal-fired Power Plants - Wet Chemical Absorption Processes. *VGB PowerTech* **2009**, *89*, 92–103.
- (9) Romeo, L. M.; Bolea, I.; Escosa, J. M. Integration of power plant and amine scrubbing to reduce CO₂ capture costs. *Appl. Therm. Eng.* **2008**, *28* (8–9), 1039–1046.
- (10) Rubin, E. S.; Chen, C.; Rao, A. B. Cost and performance of fossil fuel power plants with CO₂ capture and storage. *Energy Policy* **2007**, *35* (9), 4444–4454.
- (11) Kohl, L.; Nielsen, R. *Gas Purification*, 5th ed.; Gulf Publishing Company: Houston, TX, 1997.
- (12) Chakma, A.; Mehrotra, A. K.; Nielsen, B. Comparison of chemical solvents for mitigating CO₂ emissions from coal-fired power plants. *Heat Recovery Syst. CHP* **1995**, *15* (2), 231–240.
- (13) Pellegrini, G.; Strube, R.; Manfrida, G. Comparative study of chemical absorbents in postcombustion CO₂ capture. *Energy* **2010**, *35* (8), 851–857.
- (14) NETL. *Cost and performance baseline for Fossil Energy plants, Vol. 1: Bituminous Coal and Natural Gas to electricity*; National Energy Technology Laboratory: Pittsburgh, USA, 2010.
- (15) Gibbins, J. R.; Crane, R. I. Preliminary assessment of electricity costs for existing pulverized fuel plant retrofitted with an advanced supercritical boiler and turbine and solvent CO₂ capture. *Proc. Inst. Mech. Eng., Part A* **2004**, *218* (7), 551–555.
- (16) IEAGHG. *Improvement in power generation with post-combustion capture of CO₂*; PH4/33; IEA Greenhouse Gas R&D Program: Cheltenham, United Kingdom, 2004.
- (17) Gouedard, C.; Picq, D.; Launay, F.; Carrette, P. L. Amine degradation in CO₂ capture. I. A review. *Int. J. Greenhouse Gas Control* **2012**, *10*, 244–270.
- (18) Mertens, J.; Lepaumier, H.; Desagher, D.; Thielens, M. L. Understanding ethanolamine (MEA) and ammonia emissions from amine based post combustion carbon capture: Lessons learned from field tests. *Int. J. Greenhouse Gas Control* **2013**, *13*, 72–77.
- (19) Aroonwilas, A.; Veawab, A. Characterization and Comparison of the CO₂ Absorption Performance into Single and Blended Alkanolamines in a Packed Column. *Ind. Eng. Chem. Res.* **2004**, *43* (9), 2228–2237.
- (20) Aroonwilas, A.; Veawab, A. Integration of CO₂ capture unit using single- and blended-amines into supercritical coal-fired power plants: Implications for emission and energy management. *Int. J. Greenhouse Gas Control* **2007**, *1* (2), 143–150.
- (21) Artanto, Y.; Jansen, J.; Pearson, P.; Do, T.; Cottrell, A.; Meuleman, E.; Feron, P. Performance of MEA and amine-blends in the CSIRO PCC pilot plant at Loy Yang Power in Australia. *Fuel* **2012**, *101*, 264–275.
- (22) Puxty, G.; Rowland, R.; Allport, A.; Yang, Q.; Bown, M.; Burns, R.; Maeder, M.; Attalla, M. Carbon dioxide postcombustion capture: A novel screening study of the carbon dioxide absorption performance of 76 amines. *Environ. Sci. Technol.* **2009**, *43* (16), 6427–6433.
- (23) Schneider, R.; Schramm, H. Environmentally friendly and economic carbon capture from power plant flue gases: The SIEMENS PostCap technology. In *1st Post Combustion Capture Conference*, Abu Dhabi, 2011. Available at: <http://www.ieaghg.org>.
- (24) Oexmann, J.; Kather, A.; Linnenberg, S.; Liebenthal, U. Post-combustion CO₂ capture: Chemical absorption processes in coal-fired steam power plants. *Greenhouse Gases: Sci. Technol.* **2012**, *2* (2), 80–98.
- (25) Shen, S.; Feng, X.; Zhao, R.; Ghosh, U. K.; Chen, A. Kinetic study of carbon dioxide absorption with aqueous potassium carbonate promoted by arginine. *Chem. Eng. J.* **2013**, *222*, 478–487.
- (26) Cullinane, J. T.; Rochelle, G. R. Carbon dioxide absorption with aqueous potassium carbonate promoted by piperazine. *Chem. Eng. Sci.* **2004**, *59* (17), 3619–3630.
- (27) NETL Bench-Scale Development of a Hot Carbonate Absorption Process with Crystallization-Enabled High Pressure Stripping for Post-Combustion CO₂ Capture. Project No.: DE-FE0004360. <http://www.netl.doe.gov/> (2013).
- (28) Raynal, L.; Bouillon, P. A.; Gomez, A.; Broutin, P. From MEA to demixing solvents and future steps, a roadmap for lowering the cost of post-combustion carbon capture. *Chem. Eng. J.* **2011**, *171* (3), 742–752.
- (29) Fernandez, E. S.; Goetheer, E. L. V. DECAB: Process development of a phase change absorption process. *Energy Procedia* **2011**, *4*, 868–875.
- (30) Cousins, A.; Wardhaugh, L. T.; Feron, P. H. M. A survey of process flow sheet modifications for energy efficient CO₂ capture from flue gases using chemical absorption. *Int. J. Greenhouse Gas Control* **2011**, *5* (4), 605–619.
- (31) Le Moullec, Y.; Kanniche, M. Description and evaluation of flowsheet modifications and their interaction for an efficient monoethanolamine based post-combustion CO₂ capture. *Chem. Eng. Trans.* **2010**, *21*, 175–180, DOI: 10.3303/CET1021030.
- (32) Cousins, A.; Wardhaugh, L. T.; Feron, P. H. M. Preliminary analysis of process flow sheet modifications for energy efficient CO₂ capture from flue gases using chemical absorption. *Chem. Eng. Res. Des.* **2011**, *89* (8), 1237–1251.
- (33) Karimi, M.; Hillestad, M.; Svendsen, H. F. Capital costs and energy considerations of different alternative stripper configurations for post combustion CO₂ capture. *Chem. Eng. Res. Des.* **2011**, *89* (8), 1229–1236.

- (34) Ahn, H.; Luberti, M.; Liu, Z.; Brandani, S. Process configuration studies of the amine capture process for coal-fired power plants. *Int. J. Greenhouse Gas Control* **2013**, *16*, 29–40.
- (35) Le Moulec, Y.; Kanniche, M. Screening of flowsheet modifications for an efficient monoethanolamine (MEA) based post-combustion CO₂ capture. *Int. J. Greenhouse Gas Control* **2011**, *5* (4), 727–740.
- (36) de Miguel Mercader, F.; Magneschi, G.; Sanchez Fernandez, E.; Stienstra, G. J.; Goetheer, E. L. V. Integration between a demo size post-combustion CO₂ capture and full size power plant. An integral approach on energy penalty for different process options. *Int. J. Greenhouse Gas Control* **2012**, *11* (SUPPL), 102–113.
- (37) Sanchez Fernandez, E.; Bergsma, E. J.; de Miguel Mercader, F.; Goetheer, E. L. V.; Vlugt, T. J. H. Optimisation of lean vapour compression (LVC) as an option for post-combustion CO₂ capture: Net present value maximisation. *Int. J. Greenhouse Gas Control* **2012**, *11* (SUPPL), 114–121.
- (38) Sanchez Fernandez, E.; de Miguel Mercader, F.; Misiak, K.; van der Ham, L.; Linders, M.; Goetheer, E. L. V. New process concepts for CO₂ capture based on precipitating amino acids. *Energy Procedia* **2013**, *37*, 1160–1171.
- (39) Ahn, S.; Song, H. J.; Park, J. W.; Lee, J. H.; Lee, I. Y.; Jang, K. R. Characterization of metal corrosion by aqueous amino acid salts for the capture of CO₂. *Korean J. Chem. Eng.* **2010**, *27* (5), 1576–1580.
- (40) Aronu, U. E.; Hartono, A.; Hoff, K. A.; Svendsen, H. F. Kinetics of carbon dioxide absorption into aqueous amino acid salt: Potassium salt of sarcosine solution. *Ind. Eng. Chem. Res.* **2011**, *50* (18), 10465–10475.
- (41) Paul, S.; Thomsen, K. Kinetics of absorption of carbon dioxide into aqueous potassium salt of proline. *Int. J. Greenhouse Gas Control* **2012**, *8*, 169–179.
- (42) Kumar, P. S.; Hogendoorn, J. A.; Feron, P. H. M.; Versteeg, G. F. Equilibrium solubility of CO₂ in aqueous potassium taurate solutions: Part 1. Crystallization in carbon dioxide loaded aqueous salt solutions of amino acids. *Ind. Eng. Chem. Res.* **2003**, *42* (12), 2832–2840.
- (43) Majchrowicz, M. E.; Brilman, D. W. F.; Groeneveld, M. J. Precipitation regime for selected amino acid salts for CO₂ capture from flue gases. *Energy Procedia* **2009**, *1* (1), 979–984.
- (44) Kumar, P. S. Development and Design of Membrane Gas Absorption Processes. Ph.D. Thesis, University of Twente, The Netherlands, 2002. Available at <http://doc.utwente.nl/38284/1/t0000041.pdf>.
- (45) Kumar, P. S.; Hogendoorn, J. A.; Timmer, S. J.; Feron, P. H. M.; Versteeg, G. F. Equilibrium solubility of CO₂ in aqueous potassium taurate solutions: Part 2. Experimental VLE data and model. *Ind. Eng. Chem. Res.* **2003**, *42* (12), 2841–2852.
- (46) Goetheer, E. L. V.; Sanchez Fernandez, E. Method for depleting a flue gas of a gaseous acid compound WO2012144898 (A1); 2012.
- (47) Sanchez Fernandez, E.; Heffernan, K.; Eggink, M.; Schrama, F.; Van der Ham, L.; Linders, M.; Brilman, D. W. F.; Goetheer, E. L. V.; Vlugt, T. J. H. Conceptual design of a novel CO₂ capture process based on precipitating amino acid solvents. *Ind. Eng. Chem. Res.* **2013**, *52*, 12223–12235.
- (48) Amrollahi, Z.; Ertesvåg, I. S.; Bolland, O. Optimized process configurations of post-combustion CO₂ capture for natural-gas-fired power plant-Exergy analysis. *Int. J. Greenhouse Gas Control* **2011**, *5* (6), 1393–1405.
- (49) Aronu, U. E.; Hoff, K. A.; Svendsen, H. F. CO₂ capture solvent selection by combined absorption-desorption analysis. *Chem. Eng. Res. Des.* **2011**, *89* (8), 1197–1203.
- (50) Aronu, U. E.; Ciftja, A. F.; Kim, I.; Hartono, A. Understanding precipitation in amino acid salt systems at process conditions. *Energy Procedia* **2013**, *37*, 233–240.
- (51) Yalkowsky, S. H.; Yan, H. *Handbook of Aqueous solubility data*; CRC Press LLC: Boca Raton, FL, 2006.
- (52) Lee, J. I.; Otto, F. D.; Mather, A. E. Equilibrium between carbon dioxide and monoethanolamine solutions. *J. Appl. Chem. Biotechnol.* **1976**, *26*, 541–549.
- (53) Shen, K. P.; Li, M. H. Solubility of carbon dioxide in aqueous mixtures of monoethanolamine with methyldiethanolamine. *J. Chem. Eng. Data* **1992**, *37*, 96–100.
- (54) Knudsen, J. N. Results from test campaigns at the 1 t/h CO₂ post-combustion capture pilot-plant in Esbjerg under the EU FP7 CESAR project. In PCCCI, Abu Dhabi, 2011. Available at: <http://www.ieaghg.org>.
- (55) Wagner, W.; Kretzschmar, H. *International Steam Tables - Properties of Water and Steam based on the Industrial Formulation IAPWS-IF97*; Springer: Germany, 2008.
- (56) NIST, NIST Chemistry WebBook. In <http://webbook.nist.gov/chemistry/>.
- (57) Kumar, P. S.; Hogendoorn, J. A.; Feron, P. H. M.; Versteeg, G. F. Density, viscosity, solubility, and diffusivity of N₂O in aqueous amino acid salt solutions. *J. Chem. Eng. Data* **2001**, *46* (6), 1357–1361.
- (58) Gucker, F. T.; Allen, T. W. The Densities and Specific Heats of Aqueous Solutions of dl- α -Alanine, β -Alanine and Lactamide 1,2. *J. Am. Chem. Soc.* **1942**, *64* (2), 191–199.
- (59) Korolev, V. P.; Antonova, O. A.; Smirnova, N. L. Thermal properties and interpartical interactions of l-proline, glycine, and l-alanine in aqueous urea solutions at 288–318 K. *J. Therm. Anal. Calorim.* **2012**, *108* (1), 1–7.
- (60) Korolev, V. P.; Batov, D. V.; Smirnova, N. L.; Kustov, A. V. Amino acids in aqueous solution. Effect of molecular structure and temperature on thermodynamics of dissolution. *Russ. Chem. Bull.* **2007**, *56* (4), 739–742.